Archives of Hydro-Engineering and Environmental Mechanics
Vol. 51 (2004), No. 3, pp. 243–265

Simulation of Shear Localization in Granular Bodies within Gradient-Enhanced Hypoplasticity

Jacek Tejchman

Gdańsk University of Technology, Civil Engineering Department, 80-952 Gdańsk,
ul. Narutowicza 11/12, Poland, e-mail: tejchmk@pg.gda.pl

(Received February 18, 2004; revised July 26, 2004)

Abstract

The paper presents a FE-analysis of a spontaneous shear localization inside non-cohesive sand during plane strain compression. The calculations were carried out with a gradient-enhanced hypoplastic constitutive law. The hypoplastic law can reproduce essential features of granular bodies depending on the void ratio, pressure level and deformation direction. To model the thickness of shear zones, a characteristic length of the microstructure was incorporated via the second gradient of the modulus of the deformation rate. To determine the effect of micro-structure, the analysis was performed with different characteristic lengths for the same specimen size.

Key words: characteristic length, finite element method, gradient model, plane strain compression, shear localization

1. Introduction

Localization of deformation in the form of narrow zones of intense shearing is a fundamental phenomenon in granular materials (Vardoulakis 1977, 1980, Tejchman 1989, 1997, Tatsuoka et al 1991, 1994, Desrues et al 1996, Leśniewska 2000, Leśniewska and Mróz 2003). Thus, it is of primary importance that it be taken into account while modelling the behaviour of granulates. Localization under shear occurs, either in the interior domain in the form of spontaneous shear zones (Vardoulakis 1977, Yoshida et al 1994) or at interfaces in the form of induced shear zones where structural members are interacting and stresses are transferred from one member to the other (Uesugi et al 1988, Tejchman 1989, Hassan 1995). The localized shear zones inside the material are closely related to its unstable behaviour. Therefore, an understanding of the mechanism of the formation of shear zones is important since they act as a precursor to ultimate soil failure.

Classical constitutive models cannot describe properly both the thickness of localization zones and distances between them during numerical analyses, since

they omit the characteristic length of the microstructure. Thus, the rate boundary value problem becomes ill-posed when localization or material softening occurs, i.e. the governing differential equations of motion change the type by losing ellipticity for static and hiperbolicity for dynamic problems (Benallal et al 1987, de Borst et al 1992). This leads to such problems as zero-energy dissipation, pathological dependence on the fineness and orientation of the spatial discretization, incapability of determining the direction and size of a localized zone and non-realistic load-displacement curves. As the element mesh is refined, the width of the localized deformation decreases to a vanishing width. Thus, the solutions become meaningless. To overcome this drawback, classical constitutive models require an extension in the form of a characteristic length to regularize the rate boundary value problem and to take into account microscopic inhomogeneities triggering shear localization (e.g. size and spacing of microdefects, grain size, aggregate size, fiber spacing). Different strategies have be used to include a characteristic length in both elasto-plasticity and hypoplasticity: polar models (Mühlhaus 1989, 1990, Tejchman 1989, 2002, 2004b, de Borst et al 1992, Sluys 1992, Tejchman and Wu 1993, Tejchman et al 1999, Maier 2002), non-local models (Bazant et al 1987, Pijaudier-Cabot 1995, Brinkgreve 1994, Maier 2002, Tejchman 2003, 2004a), gradient models (Aifantis 1984, Sluys 1992, de Borst et al 1992, Pamin 1994, de Borst and Pamin 1996), and models with viscosity (Neddleman 1988, Sluys 1992, Belytschko et al 1994, Łodygowski and Perzyna 1997, Ehlers and Volk 1998). The presence of a characteristic length enables the expression of the size effect (dependence of strength and other mechanical properties on the size of the specimen) observed experimentally on softening specimens. This is made possible since the ratio l/L governs the response of the model (l – characteristic length, L – size of the structure).

The second gradient models have often been used, since the pioneering work of Aifantis (1984), Chen and Schreyer (1987) and Zbib and Aifantis (1988a, b). They have been used in damage mechanics (Peerlings et al 1998, Kuhl and Ramm 2000, Zhou et al 2002), elasticity (Triantafyllidis and Aifantis 1986), dislocation dynamics (Zbib et al 1998), plasticity (de Borst and Mühlhaus 1992, Sluys and de Borst 1994, Pamin 1994) and coupled plastic damage theories (de Borst 1998, de Borst et al 1999, Voyiadjis and Dorgan 2001). The constitutive models capture gradients in a different way. They usually involve the second gradient of the plastic strain measure (Laplacian) in the yield or potential function (plasticity) or in the damage function (damage mechanics). The plastic multiplier which is connected to the plastic strain measure is considered as a fundamental unknown and is solved at global level simultaneously with the displacement degrees of freedom (de Borst and Mühlhaus 1992, Pamin 1994, de Borst and Pamin 1996, Chen et al 2001, Aifantis 2003). In the classical theory of plasticity, the plastic multiplier is determined from an algebraic equation. Such gradient model obviously requires a C^l-continuous interpolation of the plastic multipler field. This

requirement is fulfilled by e.g. an element with the 8-nodal serendipity interpolation of displacements and 4-nodal Hermitian interpolation of plastic strain with 2×2 Gaussian integration (Pamin 1994). The extra gradient coefficient appearing in the constitutive law may be calibrated through shear band thickness measurements (Aifantis 2003).

Alternatively, all strain gradients can be taken into account (Chambon et al 2001). The stress is conjugate to the strain rate, and the so-called double stress is conjugate to its gradient. To ensure that the derivatives are continuous across two-dimensional elements boundaries, a triangular element of C^l continuity with 36 degrees of freedom developed by Dasgupta and Sengupta (1990) can be used (Zervos et al 2001, Maier 2002, Niemunis and Maier 2004). The degrees of freedom at each node are the displacements, both first order and all three second order derivatives. The model requires a relationship between the double stress and strain gradient. To simplify the calculations, Zhou et al (2002) for two-dimensional calculations used a triangular element proposed by Xia and Hutchinson (1997) with 18 DOF to take into account the first gradients of displacements for a gradient model by Fleck and Hutchinson (1993), including the entire strain gradient.

An other possibility is to modify the flow rule by introducing the second order yield function (di Prisco et al 2002, Aifantis 2003) or use the gradients of the damage variables (Fremond and Nedjar 1996).

The gradient terms can be evaluated not only by using additional (rather complex) shape functions, but also by applying an explicit method in the form of a standard central difference scheme (Alehossein and Korinets 2001, di Prisco et al 2002, Zhou et al 2002).

In this paper, a spontaneous shear localization in granular bodies was investigated with a finite element method based on a hypoplastic constitutive law extended by the second gradient of the modulus of the deformation rate. The second gradient was calculated using a standard central difference scheme (thus, additional shape functions were avoided). The advantages of this method are: simplicity of computation, little effort to modify each commercial FE-code and high computation efficiency. The FE-analysis was performed with n enhanced hypoplastic model for a specimen of dry sand subject to plane strain compression under constant lateral pressure. Similar comparative FE-calculations have already been performed within a polar hypoplasticity (Tejchman et al 1999, Tejchman 2004a, b) and non-local hypoplasticity (Tejchman 2003, 2004a) including the microstructure (related to mean grain diameter) in a different way.

2. Hypoplasticity

Hypoplastic constitutive laws (Kolymbas 1977, Gudehus 1996, Bauer 1996, von Wolffersdorff 1996, Tejchman 1997) are an alternative to elasto-plastic formulations for continuum modelling of granular materials (Lade 1977, Vermeer 1982,

Pestana and Whittle 1999). They describe the evolution of effective stress components with the evolution of strain components by a differential equation including isotropic linear and non-linear tensorial functions according to the representation theorem by Wang (1970). In contrast to elasto-plastic models, the decomposition of deformation components into elastic and plastic parts, yield surface, plastic potential, flow rule and hardening rule are not needed. The hypoplastic models describe the behaviour of so-called simple grain skeletons which are characterised by the following properties (Gudehus 1996):

- the state is fully defined through the skeleton pressure and void ratio (inherent anisotropy of contact forces between grains is not considered and vanishing principal stresses are not allowed),
- deformation of the skeleton is due to grain rearrangements (e.g. small deformations $< 10^{-5}$ due to elastic behaviour of grain contacts are negligible),
- grains are permanent (abrasion and crushing are excluded in order to keep the granulometric properties unchanged),
- three various void ratios decreasing exponentially with pressure are distinguished (minimum, maximum and critical),
- the material manifests an asymptotic behaviour for monotonous and cyclic shearing or SOM-states for proportional compression,
- rate effects are negligible,
- physico-chemical effects (capillary and osmotic pressure) and cementation of grain contacts are not taken into account.

The hypoplastic constitutive laws are of the rate type. Due to incremental non-linearity with the deformation rate, they are able describe both a non-linear stress-strain and volumetric behaviour of granular bodies during shearing up to and after the peak with a single tensorial equation. They include also: barotropy (dependence on pressure level), pycnotropy (dependence on density), dependence on the direction of deformation rate, dilatancy and contractancy during shearing with constant pressure, increase and release of pressure during shearing with constant volume, and material softening during shearing of a dense material. They are apt to describe stationary states, i.e. states in which a grain aggregate can continuously be deformed at constant stress and constant volume under a certain rate of deformation. Although, the hypoplastic models are developed without recourse to concepts of the theory of plasticity, failure surface, flow rule and plastic potential are obtained as natural outcomes (Wu and Niemunis 1996). The feature of the model is a simple formulation and procedure for determination of material parameters with standard laboratory experiments. The parameters are related to granulometric properties encompassing grain size distribution curve, shape, angularity and hardness of grains (Herle and Gudehus 1999). Owing to

that, one set of material parameters is valid within a large range of pressures and densities.

Stress changes due to the deformation of a granular body can be generally expressed by

$$\overset{o}{\sigma}_{ij} = F\left(e, \sigma_{kk}, d_{kl}\right) \tag{1}$$

wherein the Jaumann stress rate tensor (objective stress rate tensor) is defined by

$$\overset{o}{\sigma}_{ij} = \overset{\bullet}{\sigma}_{ij} - w_{ik}\sigma_{kj} + \sigma_{ik}w_{kj}, \tag{2}$$

F in Eq. 1 represents an isotropic tensor-valued function, σ_{ij} is the Cauchy skeleton (effective) stress tensor, e the void ratio and d_{kl} the rate of deformations tensor (stretching tensor). If the volume of grains remains constant (i.e. incompressible grains), the rate of the void ratio can be expressed by the evolution equation:

$$\overset{*}{e} = (1 + e)\, d_{kk}. \tag{3}$$

The rate of deformation tensor d_{ij} and the spin tensor w_{ij} are related to the material velocity v as follows:

$$d_{ij} = \left(v_{i,j} + v_{j,i}\right)/2, \quad w_{ij} = \left(v_{i,j} - v_{j,i}\right)/2, \quad ()_{,i} = \partial\,()\,/\partial x_i. \tag{4}$$

The condition of the incremental non-linearity (Bauer 1996) requires that the tensorial function F in Eq. 1 is not differentiable only for $d_{ij} = 0$. Such requirement results in the following equation where the function F is decomposed into two parts

$$\overset{o}{\sigma}_{ij} = A\left(e, \sigma_{kl}, d_{kl}\right) + B\left(e, \sigma_{ij}\right)||d_{kl}||. \tag{5}$$

The function A is linear in d_{kl}, while the function B is non-linear in d_{kl}. $||d_{kl}||$ denotes the Euclidian norm $\sqrt{d_{kl}d_{kl}}$. The following representation of the general constitutive equation is used (Gudehus 1996, Bauer 1996):

$$\overset{o}{\sigma}_{ij} = f_s\left[L_{ij}\left(\hat{\sigma}_{kl}, d_{kl}\right) + f_d N_{ij}\left(\hat{\sigma}_{ij}\right)\sqrt{d_{kl}d_{kl}}\right], \tag{6}$$

wherein the normalized stress tensor $\hat{\sigma}_{ij}$ is defined by

$$\hat{\sigma}_{ij} = \frac{\sigma_{ij}}{\sigma_{kk}}. \tag{7}$$

The scalar factors $f_s = f_s\left(e, \sigma_{kk}\right)$ and $f_d = f_d\left(e, \sigma_{kk}\right)$ take into account the influence of the density and pressure level on the stress. The stiffness factor f_s is proportional to the granulate hardness h_s and depends on the mean stress and void ratio:

$$f_s = \frac{h_s}{n h_i}\left(\frac{1+e_i}{e}\right)\left(-\frac{\sigma_{kk}}{h_s}\right)^{1-n} \tag{8}$$

with

$$h_i = \frac{1}{c_1^2} + \frac{1}{3} - \left(\frac{e_{i0}-e_{d0}}{e_{c0}-e_{d0}}\right)^{\alpha} \frac{1}{c_1\sqrt{3}}. \tag{9}$$

The granulate hardness h_s represents a density-independent reference pressure and is related to the entire skeleton (not to single grains). The density factor f_d resembles a pressure-dependent relative density index and is represented by

$$f_d = \left(\frac{e-e_d}{e_c-e_d}\right)^{\alpha}, \tag{10}$$

Here e is the current void ratio, e_c the critical void ratio, e_d denotes the void ratio at maximum densification (due to cyclic shearing), e_i the maximum void ratio, α denotes the pycnotropy coefficient, and n is the compression coefficient. The void ratio e is thus limited by e_i and e_d. The values of e_i, e_d and e_c are assumed to decrease with the pressure $p = -\sigma_{kk}/3$ according to the equations (Fig. 1):

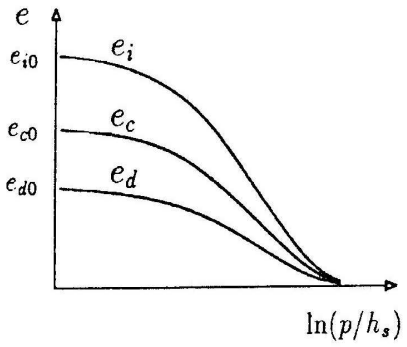

Fig. 1. Pressure dependence of void ratios

$$e_i = e_{i0}\exp[-(3p/h_s)^n], \tag{11}$$

$$e_d = e_{d0}\exp[-(3p/h_s)^n], \tag{12}$$

$$e_c = e_{c0}\exp[-(3p/h_s)^n], \tag{13}$$

wherein e_{i0}, e_{d0} and e_{c0} are the values of e_i, e_d and e_c for $\sigma_{kk} = 0$, respectively. For the tensorial functions L_{ij} and N_{ij}, the following representatives are used (Gudehus 1996, Bauer 1996, Tejchman 1997):

$$L_{ij} = a_1^2 d_{ij} + \hat{\sigma}_{ij} \hat{\sigma}_{kl} d_{kl}, \quad N_{ij} = a_1 \left(\hat{\sigma}_{ij} + \hat{\sigma}_{ij}^* \right), \tag{14}$$

where

$$a_1^{-1} = c_1 + c_2 \sqrt{\hat{\sigma}_{kl}^* \hat{\sigma}_{lk}^*} [1 + \cos(3\theta)], \tag{15}$$

$$\cos(3\theta) = -\frac{\sqrt{6}}{\left[\hat{\sigma}_{kl}^* \hat{\sigma}_{kl}^* \right]^{1.5}} \left(\hat{\sigma}_{kl}^* \hat{\sigma}_{lm}^* \hat{\sigma}_{mk}^* \right), \tag{16}$$

$$c_1 = \sqrt{\frac{3}{8}} \frac{(3 - \sin\phi_c)}{\sin\phi_c}, \quad c_2 = \frac{3}{8} \frac{(3 + \sin\phi_c)}{\sin\phi_c}. \tag{17}$$

ϕ_c is the critical angle of internal friction during stationary flow. θ denotes the Lode angle: the angle on the deviatoric plane $\sigma_1 + \sigma_2 + \sigma_3 = 0$ between the stress vector and the axis σ_3 (σ_i is the principle stress vector), and σ_{ij}^* denotes the deviatoric part of σ_{ij}. In case of sand, the hypoplastic constitutive relation is approximately valid in a pressure range 1 kPa $< -\sigma_{kk}/3 <$ 1000 kPa. Below this, additional capillary forces due to the air humidity and van der Waals forces may become important, and above it, grain crushing.

The constitutive relationship requires 7 material constants: e_{i0}, e_{d0}, e_{c0}, ϕ_c, h_s, n and α. The FE-analyses were carried out with the following material constants (for so-called Karlsruhe sand): $e_{i0} = 1.3$, $e_{d0} = 0.51$, $e_{c0} = 0.82$, $\phi_c = 30^\circ$, $h_s = 190$ MPa, $n = 0.5$ and $\alpha = 0.3$ (Bauer 1996). The parameters h_s and n are estimated from a single oedometric compression test with an initially loose specimen (h_s reflects the slope of the curve in a semi-logarithmic representation, and n its curvature, Fig. 2). The constant α is found from a triaxial test with a dense specimen (it reflects the height and position of the peak value of the stress-strain curve). The angle ϕ_c is determined from the angle of repose or measured in a triaxial test with a loose specimen. The values of e_{i0}, e_{d0}, e_{c0} are obtained with conventional index tests ($e_{c0} \approx e_{\max}$, $e_{d0} \approx e_{\min}$, $e_{i0} \approx (1.1 - 1.5) e_{\max}$. The mean grain diameter of sand is $d_{50} = 0.5$ mm.

3. Gradient Hypoplasticity

Gradient approaches have been proposed for ductile materials (metals), (Fleck and Hutchinson 1997, Chen et al 2001), quasi-brittle materials (rock, concrete)

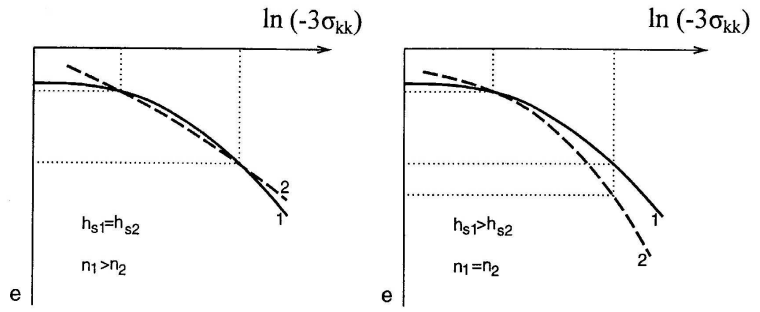

Fig. 2. Influence of n and h_s on compression curves for two different materials

(Chen and Schreyer 1987, Vardoulakis et al 1992, Pamin 1994, Meftah and Reynouard 1998, Chen et al 2001) and granular materials (Vardoulakis and Aifantis 1991, Slyus 1992, Vardoulakis and Sulem 1995, Oka et al 2001, Maier 2002, di Prisco et al 2002) to regularize a boundary value problem and to calculate localization of deformations. They include a characteristic length through the introduction of a higher order spatial gradient of different constitutive variables (elastic, plastic, damage, hypoplastic) in the governing equations of material description. The higher-order deformation gradients give rise to a non-local effect which regularizes the localization of deformation and renders numerical analyses mesh-objective. The gradient terms are thought to reflect the fact that below a certain size scale the interaction between the micro-structural carriers of the deformation is non-local (Aifantis 2003). They disappear from the constitutive model if a homogeneous state of strain and stress is analyzed. Thus, they can be treated as a singular perturbation of the standard equations (Askes et al 2001).

The advantage of a gradient approach is that it is suitable for both shear and tension (decohesion) dominated applications. The disadvantages are: necessity of use of complex shape functions (Pamin 1994, Chen et al 2001) and the characteristic length is not directly related to the grain or aggregate diameter (granulates and concrete).

Gradient–type regularization can be derived from non-local models (Bazant et al 1987) which are based on spatial averaging of state variables (strains, stresses, plastic strain measure, damage measure) in a certain neighbourhood of a given state. Each non-local state variable Y^* can be calculated in point x as (Bazant et al 1987):

$$Y^*(x) = \frac{1}{A}\int_{-\infty}^{\infty} w(r)\, Y(x+r)\, dV, \tag{18}$$

where r is the distance from the material point compared to other points of the entire material body, w is the weighting function, Y is local state variable, V denotes the volume and A is the weighted body area:

$$A = \int_{-\infty}^{\infty} w(r)\, dV. \tag{19}$$

As the weighting function w, the error density function is usually chosen (Brinkgreve 1994, Maier 2002):

$$w(r) = \frac{1}{l\sqrt{\pi}} e^{-(r/l)^2}. \tag{20}$$

The parameter l denotes a characteristic length (it determines the size of the neighbourhood influencing the state at the given point). At the distance of a few times the length l, the function w is equal to zero (Fig. 3). The characteristic length l in Eq. 20 can be related to dimensions of the material micro-structure on the basis of comparative calculations on localization of deformation (Tejchman 2003).

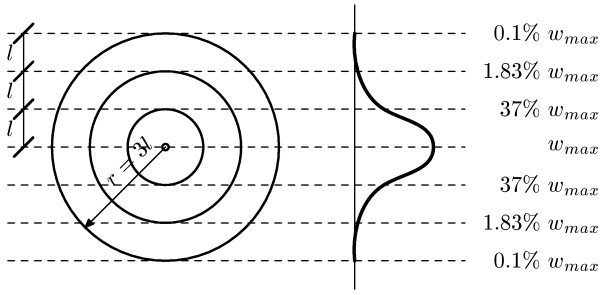

Fig. 3. Distribution of the weighting function w

By expanding the state variable $Y(x + r)$ in Eq. 18 into a Taylor series around the point $r = 0$, choosing the error function w (Eq. 20) as the weighting function and neglecting terms higher than second order, the following relationship is obtained for a non-local gradient variable (one-dimensional problems), (Brinkgreve 1994, Pamin 1994)

$$Y^*(x) = \frac{1}{A}\left[\int_{-\infty}^{\infty} \frac{1}{l\sqrt{\pi}} e^{-(r/l)^2} Y(x)dr + \int_{-\infty}^{\infty} \frac{r}{l\sqrt{\pi}} e^{-(r/l)^2} \frac{dY(x)}{dx} dr + \right.$$
$$+ \int_{-\infty}^{\infty} \frac{r^2}{2l\sqrt{\pi}} e^{-(r/l)^2} \frac{d^2Y(x)}{dx^2} dr + \int_{-\infty}^{\infty} \frac{r^3}{6l\sqrt{\pi}} e^{-(r/l)^2} \frac{d^3Y(x)}{dx^3} dr + \qquad (21)$$
$$\left. + \int_{-\infty}^{\infty} \frac{r^4}{24l\sqrt{\pi}} e^{-(r/l)^2} \frac{d^4Y(x)}{dx^4} dr + ... \right] = Y + l\frac{\partial Y}{\partial x} + \frac{l^2}{4}\frac{\partial^2 Y}{\partial x^2}.$$

The odd derivative can be cancelled because of the implicit assumption of isotropy (de Borst et al 1992). Restricting the treatment to the second-order derivative, each non-local state variable is equal to

$$Y^*(x) = Y + \frac{l^2}{4}\frac{\partial^2 Y}{\partial x^2}. \qquad (22)$$

In the FE-calculations, the second gradient of the modulus of the deformation rate (Eq. 6)

$$d = \sqrt{d_{kl} d_{kl}} \qquad (23)$$

was taken into account. This parameter is always positive and strongly affected by shear localization (Tejchman 2003, 2004a). Thus, the enhanced (non-local) modulus of the deformation rate d^* was calculated for two-dimensional problems in the following way

$$d^*(x, y) = d + \frac{l^2}{4}\left(\frac{\partial^2 d}{\partial x^2} + \frac{\partial^2 d}{\partial y^2} + 2\frac{\partial^2 d}{\partial x \partial y}\right). \qquad (24)$$

Alternatively, the enhanced (non-local) density factor f_d of Eq. 10 can be used (Tejchman 2003).

Instead of using complex shape functions to describe the evolution of the second gradient of d, a standard central difference scheme was applied (Alehossein and Korinets 2001, di Prisco et al 2002, Zhou et al 2002) which assumes a parabolic interpolation of the function d^* (the variable d is influenced by the values only in adjacent elements). From the theory of finite difference method, for the variable d^* (when the difference paces dx and dy are infinitesimal) the second derivatives can be approximated in each element (when the mesh is regular in the vertical and horizontal direction) according to Fig. 4 as:

$$\frac{\partial^2 d_5}{\partial x^2} = \frac{d_8 - 2d_5 + d_2}{dx^2}, \qquad (25)$$

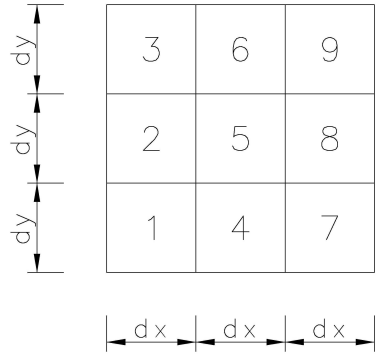

Fig. 4. Diagram for determination of the gradient of the constitutive variable for each triangular element

$$\frac{\partial^2 d_5}{\partial y^2} = \frac{d_6 - 2d_5 + d_4}{dy^2}, \tag{26}$$

$$\frac{\partial^2 d_5}{\partial x\,\partial y} = \frac{d_9 + d_1 - d_3 - d_7}{4dxdy}, \tag{27}$$

where the lower subscript at d denotes the number of the element. Thus, the effect of adjacent elements can be taken into account in each element (e.g. the element "5" of Fig. 4). The higher order polynomial interpolation of the function $d^*(x, y)$ can also be assumed.

One must keep in mind that the first order gradients in Eq. 21 cannot be omitted under certain circumstances, e.g. in pure bending and indentation processes (Chen et al 2001).

4. FE-Implementation

FE-calculations of plane strain compression tests were performed with a sand specimen which was $h_o = 10$ cm high and $b = 2$ cm wide. Only quadrilateral finite elements composed of four diagonally crossed triangles were applied, to avoid volumetric locking. In total, 320 quadrilateral elements (0.25×0.25 cm^2) divided into 1280 triangular elements with linear shape functions for displacements were used. The dimensions of finite elements were $5 \times d_{50}$ to obtain the thickness of shear zones independent of the mesh size within an extended hypoplasticity (Tejchman 1997, Tejchman et al 1999, Maier 2002). Integration was performed with one sampling point placed in the middle of each element. The calculations were carried out with small deformations. The second gradients of the variable d were calculated in each triangular element (Eqs. 25–27, Fig. 4) on the basis of the previous iteration step (explicit scheme).

As the initial stress state, a K_0-state with $\sigma_{22} = \sigma_c + \gamma_d x_2$ and $\sigma_{11} = \sigma_c + K_0 \gamma_d x_2$ was assumed in the sand specimen where σ_c denotes the confining pressure, x_2 is the vertical coordinate measured from the top of the specimen, γ_d denotes the initial volume weight and $K_0 = 0.47$ is the earth pressure coefficient at rest (σ_{11} – horizontal normal stress, σ_{22} – vertical normal stress).

A quasi-static deformation in sand was initiated through a constant vertical displacement increment prescribed at nodes along the upper edge of the specimen. The boundary conditions of the sand specimen were: no shear stress at the top and bottom. To preserve the stability of the specimen against horizontal sliding along the top boundary, the node in the middle of the bottom was kept fixed. Along all boundaries, all derivatives of the modulus of the deformation rate (Eq. 24) were set at zero analogously to elasto-plastic FE-solutions where the derivative of the plastic multiplier is assumed to be zero at boundaries (Pamin 1994, de Borst and Pamin 1996).

To obtain a shear zone inside the specimen, a weaker element with a high initial void ratio, $e_0 = 0.90$, was inserted at mid-point of the specimen.

For the solution of a non-linear system, a modified Newton-Raphson scheme with line search was used with a global stiffness matrix calculated with only first term of the constitutive equations (linear in d_{kl}). The stiffness matrix was updated every 100 steps. To accelerate the calculations in the softening regime, the initial increments of displacements in each calculation step were assumed to be equal to the final increments in the previous step. The iteration steps were performed using translational convergence criteria.

The gradient hypoplastic constitutive model was implemented in the author's finite element code.

5. FE-Results

5.1. Classical Continuum

Figures 5 and 6 present the results of plane strain compression with dense sand ($e_o = 0.60$) within a conventional (local) continuum (Eqs. 1–17) under confining pressure $\sigma_c = 0.2$ MPa (Tejchman 2003). The normalized load-displacement curve is depicted in Fig. 5a. Figure 5b shows the deformed FE-mesh with the distribution of void ratio. The darker the region, the higher the void ratio. The evolution of the void ratio e, density factor f_d (Eq. 10), modulus of the deformation rate d (Eqs. 6) and Lode angle θ (Eq. 16) at two different locations: inside the shear zone and far beyond it are demonstrated in Fig. 6.

The resultant vertical force on the specimen top P increases first, shows a pronounced peak, drops later and reaches a residual state (Fig. 5a). The overall angle of internal friction for the sand specimen, calculated from Mohr's formula

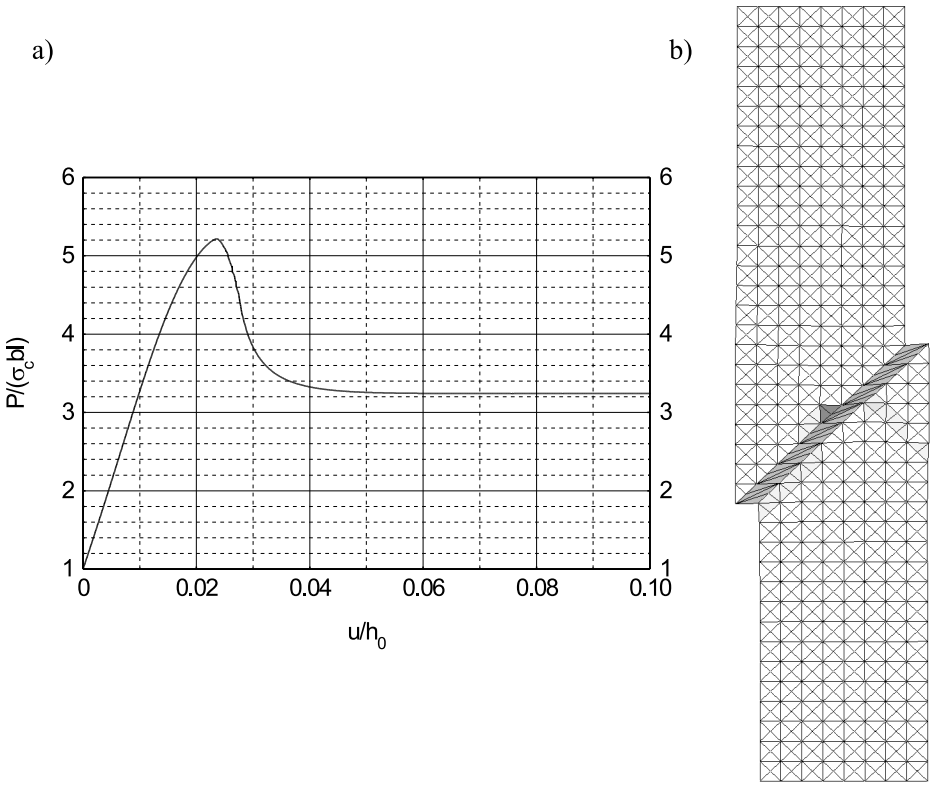

Fig. 5. Load-displacement curve and deformed FE-mesh with the distribution of void ratio in the residual state (local continuum, $e_o = 0.60$, $\sigma_c = 0.2$ MPa)

$$\phi = \arcsin \frac{\sigma_1 - \sigma_3}{\sigma_1 + \sigma_3} \tag{28}$$

is equal to $\phi_p = 42.7^{\circ}$ at peak ($u/h_0 = 2.36\%$). At residual state, it is equal to $\phi_{cr} = 32.0^{\circ}$ ($u/h_0 \cong 5\%$). In Eq. 28, $\sigma_1 = P/(bl)$ denotes the vertical principle stress, $\sigma_3 = \sigma_c$ is the horizontal principal stress, $b = 0.02$ m is the specimen width, $l = 1.0$ m (due to two-dimensional calculations) and u denotes the vertical displacement of the top.

At the beginning of the compression process, two intersecting shear zones emerge expanding outward from the weakest element in the middle of the specimen (Tejchman 2004b). Afterwards, and up to the end, only one shear zone dominates. The complete shear zone is already noticeable shortly after the peak. It is characterized by both a concentration of shear deformations, and a significant increase of the void ratio and modulus of the deformation rate. The calculated thickness of the shear zone is equal to the width of finite elements and its inclination to the mesh orientation (Fig. 5b).

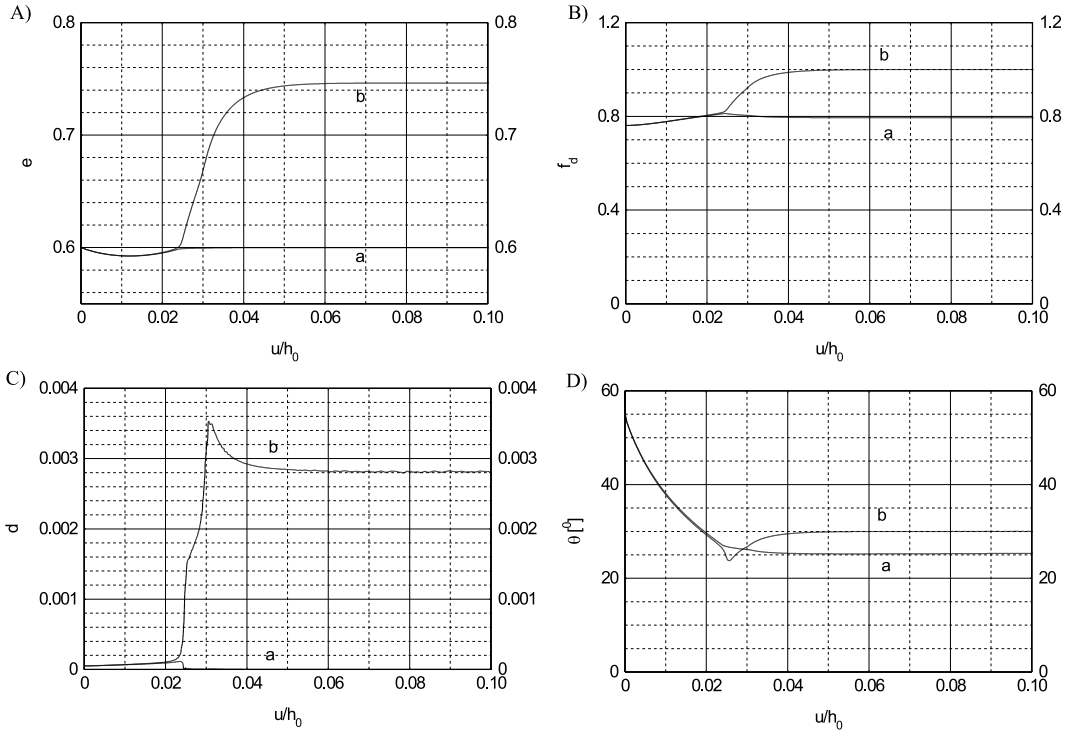

Fig. 6. Evolution of void ratio e (A), density factor f_d (B), modulus of the deformation rate d (C) and Lode angle θ (D) (a – outside the shear zone, b – in the shear zone)

The void ratio e at the beginning decreases (up to $u/h_0 = 1\%$) and afterwards increases in the whole specimen (Fig. 6A). In the shear zone, it reaches a pressure-dependent critical value at residual state ($e = e_c = 0.745$, Eq. 13). Beyond the shear zone, the void ratio reaches the initial value. The thickness of the shear zone on the basis of an increase of the void ratio is slightly larger, since a dense granular material already dilates before a shear zone forms.

The density factor f_d (Eq. 10) continuously increases in the whole specimen (Fig. 6B). At residual state, it is equal to 1.0 (shear zone) and 0.8 (remaining region).

The modulus of the deformation rate d increases uniformly in the whole specimen at the beginning of loading, to $u/h_0 = 2.2\%$. Later, it is significant only in the shear zone (Fig. 6C). It increases strongly in the range of $u/h_0 = 2 - 3\%$. Afterwards, it decreases and approaches an asymptote. On the basis of the difference between the modulus of the deformation rate in the shear zone and beyond it, one can find that the shear zone occurs before the peak of the load-displacement curve at $u/h_0 = 2.2\%$.

The Lode angle θ (Eq. 13) is equal to 30° in the shear zone and 25° beyond the shear zone (residual state), Fig. 6D.

5.2. Gradient Continuum

The results with the modulus of the deformation rate enhanced by its second gradient d^* (Eq. 24) for dense sand ($e_o = 0.60$, $\sigma_c = 0.2$ MPa) are shown in Figs. 7–12.

The greater the characteristic length, the greater both the maximum normalized vertical force on the top, and the greater the vertical displacement of the top corresponding to the peak and residual force (Figs. 7 and 9). The material becomes more ductile with increasing l. The size effect due to l/L ($L = h_0$) is for dense sand almost linear (Fig. 9). In reality, this effect could be greater due to the fact that the characteristic length influences the material properties (e.g. the larger mean grain diameter, the greater both the maximum internal friction and dilatancy angles). The mean angles of internal friction for the entire sand specimen are equal to $\phi_p = 42.8^\circ - 43.3^\circ$ (at peak). The residual internal friction angle, 32.2°, is not influenced by l in the investigated range.The obtained results of internal friction angles at peak and in the residual state in dense sand, and the corresponding vertical displacements of the sand specimen compare well with experimental results with Karlsruhe sand carried out by Vardoulakis and Goldscheider (1981), Fig. 13. In the plane strain compression tests by Vardoulakis and Goldscheider (1981) the dimension of the specimen were: $h_0 = 140$ mm, $b = 40$ mm and $l = 80$ mm. The experiments with very dense sand ($e_o = 0.55$) resulted in $\phi_p = 45.0^o$ and $\phi_{cr} = 32.9^o$ at $\sigma_c = 200$ kPa. The shape of the calculated load-displacement curves is close to the experimental one. However, the calculated stiffness is too high before the peak (in the hardening region).

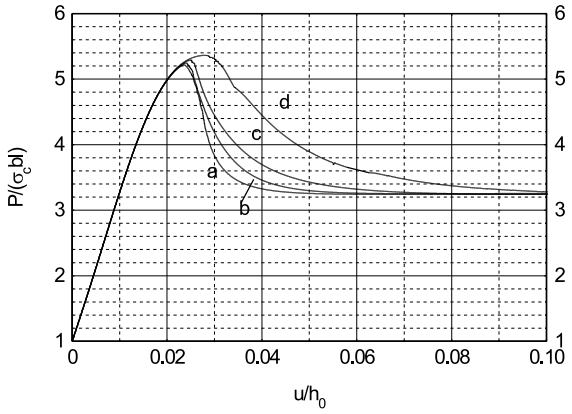

Fig. 7. Normalized load-displacement curves (gradient continuum, $e_o = 0.60$, $\sigma_c = 0.2$ MPa): a) $l = 0.0$ mm,b) $l = 0.5$ mm, c) $l = 1.0$ mm, d) $l = 2.0$ mm

The thickness of the internal shear zone grows with increasing l and is (on the basis of shear deformation): $t_{sz} \cong 5.5$ mm $= 11 \times l$ ($l = 0.5$ mm), $t_{sz} \cong 7.3$

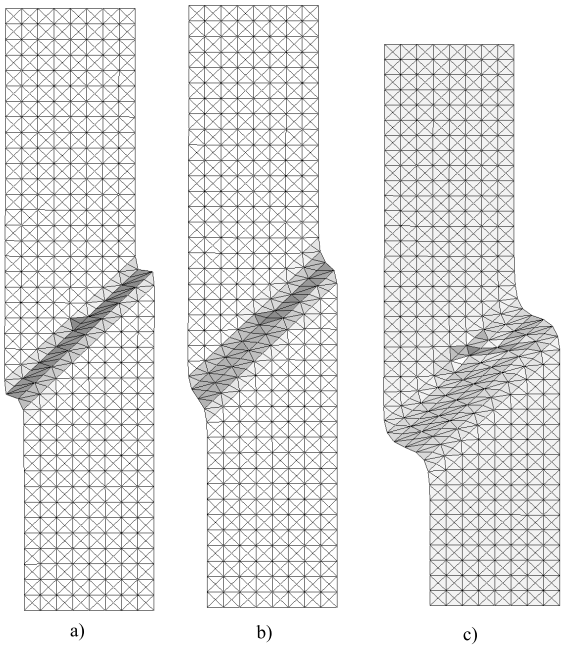

Fig. 8. Deformed FE-meshes with the distribution of void ratio at residual state at $u/h_0 = 5\%$ (a, b) and $u/h_0 = 10\%$ (c) (gradient continuum, $e_o = 0.60$, $\sigma_c = 0.2$ MPa): a) $l = 0.5$ mm, b) $l = 1.0$ mm, c) $l = 2$ mm

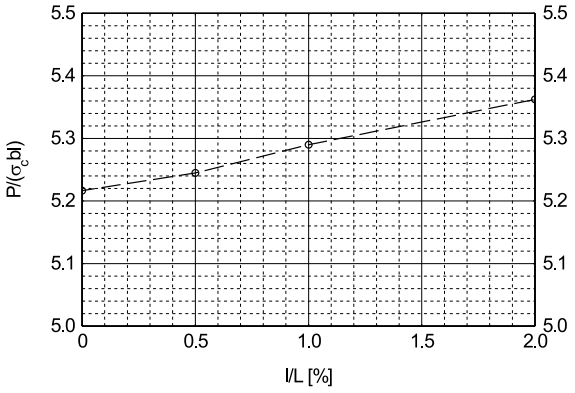

Fig. 9. Relationship between the normalized maximum vertical load $P/\sigma_c bl$) and the ratio (l/L)

mm $\cong 7 \times l$ ($l = 1.0$ mm) and $t_{sz} \cong 11.2$ mm $\cong 5 \times l$ ($l = 2.0$ mm), Fig. 8. If the characteristic length is greater than $l = 2.5$ mm, the shear zone does not appear and the diffuse deformations are concentrated at the bottom of the specimen. The calculated thickness of the shear zone in dense Karlsruhe sand with $l = 1$ mm is in accordance with the observed thickness during experiments at $\sigma_c =$ 200 kPa: $t_{sz} = 13 \times d_{50}$ (Vardoulakis 1977, 1980, Vardoulakis and Goldscheider 1981) and $10 \times d_{50}$ (Yoshida et al 1994) ($d_{50} = 0.4 - 0.5$). Thus, one can assume that the characteristic length of the gradient continuum is equal to two mean grain diameters in the case of Karlsruhe sand i.e. $l \cong 2 \times d_{50}$ (as in the non-local hypoplastic continuum, Tejchman 2003, 2004a). The thickness of the shear zone is not affected by the mesh size (Fig. 14). The results of Fig. 14 were obtained with the FE-mesh consisting of 1280 quadrilateral elements (0.125×0.125 cm^2) divided into 5120 triangular elements.

The void ratio (Fig. 10) and the density factor (Fig. 11) in the shear zone are slightly smaller in the residual state than in the conventional continuum (Figs. 6A and 6B): $e = 0.742$ and $f_d = 0.987$.

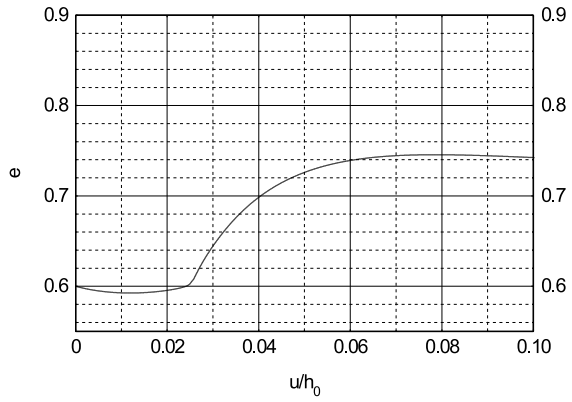

Fig. 10. Evolution of void ratio e inside the shear zone (gradient continuum, $l = 1.0$ mm, $e_o = 0.60$, $\sigma_c = 0.2$ MPa)

On the basis of the evolution of the gradient modulus of deformation in the shear zone (Fig. 12) at the beginning of loading, one can deduce that the shear zone occurs slightly before the peak of the vertical force on the top at $u/h_0 = 2.2\%$ (the peak value appears at $u/h_0 = 2.5\%$ with $l = 1$ mm). The second gradient of d becomes noticeable only in the shear zone during softening. After the peak, the enhanced modulus d^* is smaller than the local one d.

Compared to non-local (Tejchman 2003, 2004a) and polar (Tejchman et al 1999, Tejchman 2004b) numerical analyses, the gradient theory provides similar robust FE-results. However, it requires less computation time than the non-local one and is easier to implement than the polar one.

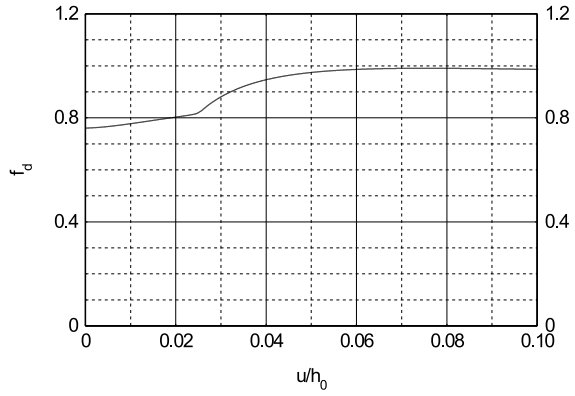

Fig. 11. Evolution of density factor f_d inside the shear zone (gradient continuum, $l = 1.0$ mm, $e_o = 0.60$, $\sigma_c = 0.2$ MPa)

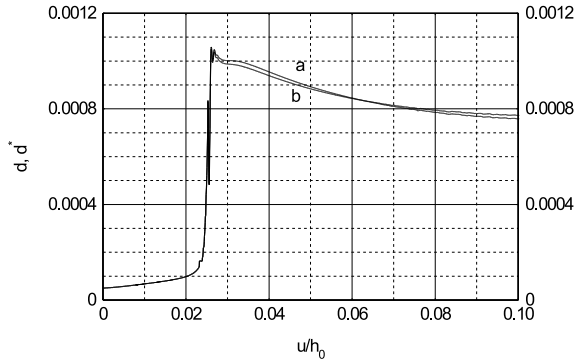

Fig. 12. Evolution of the modulus of the deformation rate d (a) and d^* (b) in the shear zone (gradient continuum, $l = 1.0$ mm, $e_o = 0.60$, $\sigma_c = 0.2$ MPa)

6. Conclusions

The FE-calculations of a plane strain compression test for granular materials demonstrate that the mesh dependence inherent in classical plasticity is remedied using the gradient approach allowing for robust localization computations.

The gradient hypoplastic model provides full regularization of the boundary value problem during plane strain compression.

The normalized vertical force on the top increases linearly with increasing characteristic length (using the same parameters as other material).

The thickness of the localized shear zone increases with increasing characteristic length.

The characteristic length of the gradient approach can be calibrated for different sands with a numerical analysis of a laboratory plane strain compression test.

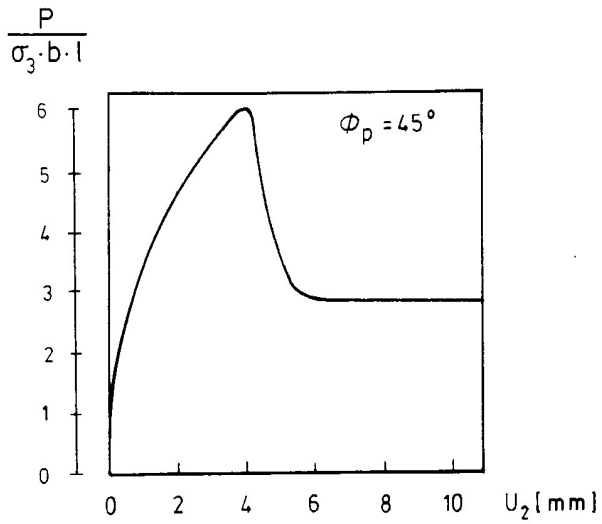

Fig. 13. Experimental load-displacement curve from a plane strain compression test (Vardoulakis and Goldscheider 1981) (σ_3 – lateral pressure, u_2 – vertical displacement of the top surface)

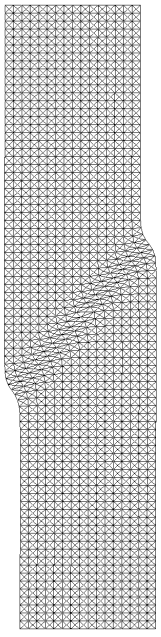

Fig. 14. Deformed FE-mesh at residual state at $u/h_0 = 5\%$ (dense mesh, gradient continuum, $e_o = 0.60$, $\sigma_c = 0.2$ MPa)

References

Aifantis E. (1984), On the Microstructural Origin of Certain Inelastic Models, *Trans. ASME J. Mat. Engng. Technol.*, 106, 326–330.

Aifantis E. (2003), Update on Class of Gradient Theories, *Mechanics of Materials* 35, 259–280.

Alehossein H., Korinets A. (2001), Gradient Dependent Plasticity and the Finite Difference Method, in: *Bifurcation and Localisation Theory in Geomechanics* (H. B. Mühlhaus et al, eds), Swets and Zeitlinger, Lisse, 117–124.

Askes H., Suiker A. S. J., Sluys L. J. (2001), Dispersion Analysis and Numerical Simulations of Second-Order and Fourth-Order Strain Gradient Models Based on a Microstructure, *Proc. ECCM-2001,* Cracow, Poland, 1–20.

Bauer E. (1996), Calibration of a Comprehensive Hypoplastic Model for Granular Materials, *Soils and Foundations*, 36, 1, 13-26.

Bazant Z., Lin F., Pijaudier-Cabot G. (1987), Yield Limit Degradation: Non-Local Continuum Model with Local Strain, *Proc. Int. Conf. Computational Plasticity,* Barcelona. In: Owen, editor, 1757–1780.

Belytschko T., Chiang H., Plaskacz E. (1994), High Resolution Two Dimensional Shear Band Computations: Imperfections and Mesh Dependence, *Com. Meth. Appl. Mech. Engng.*, 119, 1–15.

Benallal A., Billardon R., Geymonat G. (1987), Localization Phenomena at the Boundaries and Interfaces of Solids, *Proc. of the 3rd Int. Conf. Constitutive Laws for Engineering Materials: Theory and Applications,* Tucson, Arizona. In: C. S. Desai et al, editors, 387–390.

Borst R. de, Mühlhaus H. B. (1992), Gradient dependent plasticity: formulation and algorithmic aspects, *Int. J. Numer. Methods Engng.*, 35, 521–539.

Borst R. de, Mühlhaus H. B., Pamin J., Sluys L. (1992), Computational Modelling of Localization of Deformation, *Proc. of the 3rd Int. Conf. Comp. Plasticity*, In: D. R. J. Owen, H. Onate, E. Hinton, eds., Swansea, Pineridge Press, 483–508.

Borst R. de, Pamin J. (1996), Some Novel Developments in Finite Element Procedures for Gradient-Dependent Plasticity, *Int. J. Numer. Meth. Eng.*, 39 (14), 2477–2502.

Borst R. de (1998), On Gradient-Enhanced Coupled Plastic Damage Theories, in: *Computational Mechanics* (S. Idelsohn, E. Onate, E. Dvorkin, eds.), Barcelona, Spain.

Borst R. de, Pamin J., Geers M. G. D. (1999), On Coupled Gradient Theory, *Eur. J. Mech. A-Solid* 18, 6, 939–962.

Brinkgreve R. (1994), *Geomaterial Models and Numerical Analysis of Softening*, Dissertation, Delft University, 1–153.

Chambon R., Caillerie D., Matsuchima T. (2001), Plastic Continuum with Microstructure, Local Second Gradient Theories for Geomaterials: Localization Studies, *Int. J. Solids and Structures,* 38, 8503–8527.

Chen J., Yuan H., Kalkhof D. (2001), A Non-Local Damage Model for Elastoplastic Materials Based on Gradient Plasticity Theory, *Bericht Paul Scherrer Institut*, 1–130.

Chen Z., Schreyer H. L. (1987), Simulation of Soil-Concrete Interfaces with Non-Local Constitutive Models, *J. Engng. Mech.*, 113, 1665–1677.

Dasgupta S., Sengupta D. (1990), A Higher Order Triangular Plate Bending Element – Dependent Plasticity and Damage Revisited, *Int. J. Num. Meth. Engng.*, 30, 419–430.

Desrues J., Chambon R., Mokni M., Mazerolle F. (1996), Void ratio evolution inside shear bands in triaxial sand specimens studied by computed tomography, *Géotechnique,* 46, 3, 529–546.

Ehlers W., Volk W. (1998), Fundamental Considerations on the Numerical Investigation of Shear Band Phenomena in Saturated and Non-Saturated Frictional Porous Materials, *Computational Mechanics – New Trends and Applications.* In: S. Idelsohn, E. Onate, E. Dworkin, editors, CIMNE Barcelona, 1–21.

Fleck N. A., Hutchinson J. W. (1993), A Phenomenological Theory for Strain Gradient Effects in Plasticity, *J. Mechanics and Physics of Solids*, 41, 12, 1825–1857.

Fleck N. A., Hutchinson J. W. (1997), Strain Gradient Plasticity, *Adv. Appl. Mech.*, 33, 295–361.

Fremond M., Nedjar B. (1996), Damage, Gradient of Damage and Principle of Virtual Power, *I. J. Solids and Structures,* 33, 8, 1083–1103.

Gudehus G., (1996), A Comprehensive Constitutive Equation for Granular Materials, *Soils and Foundations,* 36, 1, 1–12.

Hassan A. H. (1995), *Etude Experimentale et Numerique du Comportement Local et Global d'une Interface Sol Granulaire Structure,* Dissertation, Grenoble University.

Herle I., Gudehus G. (1999), Determination of Parameters of a Hypoplastic Constitutive Model from Grain Properties, *Mechanics of Cohesive-Frictional Materials*, 4, 5, 461–486.

Kolymbas D. (1977), A Rate-Dependent Constitutive Equation for Soils, *Mech. Res. Comm.*, 6, 367–372.

Kuhl E., Ramm E. (2000), Simulation of Strain Localization with Gradient Enhanced Damage Models, *Computational Materials Sciences*, 16, 176–185.

Lade P. V. (1977), Elasto-Plastic Stress-Strain Theory for Cohesionless Soil with Curved Yield Surfaces, *Int. J. Solid Structures.*, 13, 1019–1035.

Leśniewska D. (2000), *Analysis of Shear Band Pattern Formation in Soil, Habilitation,* Institute of Hydro-Engineering of the Polish Academy of Sciences, Gdańsk.

Leśniewska D., Mróz Z. (2003), Shear Bands in Soil Deformation Processes, in: *Bifurcations and Instabilities in Geomechanics* (J. Labuz and A. Drescher, eds), Swets and Zeitlinger, 109–119.

Łodygowski P. V., Perzyna P. (1997), Numerical Modelling of Localized Fracture of Inelastic Solids in Dynamic Loading Process, *Int. J. Num. Meth. Eng.*, 40, 22, 4137–4158.

Maier T. (2002), *Numerische Modellierung der Entfestigung im Rahmen der Hypoplastizität,* PhD Thesis, University of Dortmund.

Meftah F., Reynouard J. M. (1998), A Multilayered Mixed Beam Element in Gradient Plasticity for the Analysis of Localized Failure Mode, *Mechanics of Cohesive-Frictional Materials*, 3, 305–322.

Mühlhaus H.-B. (1989), Application of Cosserat Ttheory in Numerical Solutions of Limit Load Problems, *Ing. Arch.*, 59, 124–137.

Mühlhaus H.-B. (1990), Continuum Models for Layered and Blocky Rock, *Comprehensive Rock Engineering*, In: J. A. Hudson, Ch. Fairhurst, editors, 2, 209–231, Pergamon Press.

Neddleman A. (1998), Material Rate Dependence and Mesh Sensitivity in Localization Problems, *Comp. Meths. Appl. Mech. Eng.*, 67, 69–85.

Niemunis A., Maier T. (2004), Towards Gradient Continuum with Hypoplastic Model (under preparation).

Oka F., Jing M., Higo Y. (2001), Effect of Transport of Pore Water on Strain Localisation Analysis of Fluid-Saturated Strain Gradient Dependent Viscoplastic Geomaterial, in: *Bifurcation and Localisation Theory in Geomechanics* (H. B. Mühlhaus et al, eds), Swets and Zeitlinger, Lisse, 77–83.

Pamin J. (1994), *Gradient Dependent Plasticity in Numerical Simulation of Localisation Phenomena,* PhD Thesis, Delft University.

Peerlings R. H. J., Borst R. de, Brekelmans W. A. M., Geers M. G. D. (1998), Gradient-Enhanced Damage Modelling of Concrete Fracture, *Mechanics of Cohesive-Frictional Materials*, 3, 323–342.

Pestana J. M., Whittle A. J. (1999), Formulation of a Unified Constitutive Model for Clays and Sands, *Int. J. Num. Anal. Meth. Geomech.*, 23, 1215–1243.

Pijaudier-Cabot G. (1995), Non Local Damage, *Continuum Models for Materials with Microstructure.* In: H. B. Mühlhaus, editor, John Wiley & Sons Ltd, 105–143.

Prisco C. di, Imposimato S., Aifantis E. C. (2002), A Visco-Plastic Constitutive Model for Granular Soils Modified According to Non-Local and Gradient Approaches, *Int. J. Num. and Anal. Meth. Geomech.,* 26, 121–138.

Sluys L. Y. (1992), *Wave Propagation, Localisation and Dispersion in Softening Solids,* PhD Thesis, Delft University of Technology.

Sluys L. J., Borst R. de (1994), Dispersive Properties of Gradient and Rate-Dependent Media, *Mech. Mater.*, 183, 131–149.

Tatsuoka F., Okahara M., Tanaka T., Tani K., Morimoto T., Siddiquee M. S. (1991), Progressive Failure and Particle Size Effect in Bearing Capacity of Footing on Sand, *Proc. of the ASCE Geotechnical Engineering Congress,* 27, 2, 788–802.

Tatsuoka F., Siddiquee M. S., Yoshida T., Park C. S., Kamegai Y., Goto S., Kohata Y. (1994), Testing Methods and Results of Element Tests and Testing Conditions of Plane Strain Model Bearing Capacity Tests using Air-Dried Dense Silver Buzzard Sand, *Internal Report,* University of Tokyo, 1–129.

Tejchman J. (1989), Scherzonenbildung und Verspannungseffekte in Granulaten unter Berücksichtigung von Korndrehungen, *Publication Series of the Institute of Soil and Rock Mechanics*, University Karlsruhe, 117, 1–236.

Tejchman J., Wu W. (1993), Numerical Study on Shear Band Patterning in a Cosserat Continuum, *Acta Mechanica,* 99, 61–74.

Tejchman J. (1997), Modelling of Shear Localisation and Autogeneous Dynamic Effects in Granular Bodies, *Publication Series of the Institute for Soil and Rock Mechanics,* University Karlsruhe, 140.

Tejchman J., Herle I., Wehr J. (1999), FE-Studies on the Influence of Initial Void Ratio, Pressure Level and Mean Grain Diameter on Shear Localization, *Int. J. Num. Anal. Meth. Geomech.,* 23, 15, 2045–2074.

Tejchman J. (2002), Patterns of Shear Zones in Granular Materials within a Polar Hypoplastic Continuum, *Acta Mechanica*, 155, 1–2, 71–95.

Tejchman J. (2003), A Non-Local Hypoplastic Constitutive Law to Describe Shear Localisation in Granular Bodies, *Archives of Hydro-Engineering and Environmental Mechanics*, 50, 4, 229–250.

Tejchman J. (2004a), Comparative FE-Sof Shear Localizations in Granular Bodies within a Polar and Non-Local Hypoplasticity, *Mechanics Research Communications*, 31/3, 341–354.

Tejchman J. (2004b), Effect of Heterogeneity on Shear Zone Formation During Plane Strain Compression, *Archives of Hydro-Engineering and Environmental Mechanics,* 51, 2, 149–183.

Triantafyllidis N., Aifantis E. C. (1986), A Gradient Approach to Localization of Deformation, Hyperelastic Materials, *J. Elasticity* 16, 225–238.

Uesugi M., Kishida H., Tsubakihara Y. (1988), Behaviour of Sand Particles in Sand-Steel Friction, *Soils and Foundations*, 28, 1, 107–118.

Vardoulakis I. (1977), *Scherfugenbildung in Sandkörpern als Verzweigungsproblem,* Dissertation, Institute for Soil and Rock Mechanics, University of Karlsruhe, 70.

Vardoulakis I. (1980), Shear Band Inclination and Shear Modulus in Biaxial Tests, *Int. J. Num. Anal. Meth. Geomech.,* 4, 103–119.

Vardoulakis I., Goldscheider M. (1981), Biaxial Apparatus for Testing Shear Bands in Soils, *Proc. 10^h Conf. Soil Mech. Found. Engng.*, Stockholm, 819–824.

Vardoulakis I., Aifantis E. (1991), A Gradient Flow Theory of Plasticity for Granular Materials, *Acta Mechanica* 87, 197–217.

Vardoulakis I., Shah K. R., Papanastasiou P. (1992), Modelling of Tool-Rock Shear Interfaces using Gradient-Dependent Flow Theory of Plasticity, *Int. J. Rock Mech. Min. Sci. Geomech.*, 29, 6, 573-582.

Vardoulakis I., Sulem J. (1995), *Bifurcation Analysis in Geomechanics*, Blackie Academic and Professional, Glasgow.

Vermeer P. (1982), A Five-Constant Model Unifying Well-Established Concepts, *Proc. Int. Workshop on Constitutive Relations for Soils* (eds. G. Gudehus, F. Darve, I. Vardoulakis), Balkema, 175–197.

Voyiadjis G. Z., Dorgan R. J. (2001), Gradient Formulation in Coupled Damage-Plasticity, *Arch. of Mech.*, 53, 565–597.

Wang C. C. (1970), A New Representation Theorem for Isotropic Functions, *J. Rat. Mech. Anal.*, 36, 166–223.

Wolffersdorff P. A. von (1996), A Hypoplastic Relation for Granular Materials with a Predefined Limit State Surface, *Mechanics Cohesive-Frictional Materials,* 1, 251–271.

Wu W., Niemunis A. (1996), Failure Criterion, Flow Rule and Dissipation Function Derived from Hypoplasticity, *Mechanics of Cohesive-Frictional Materials*, 1, 145–163.

Xia Z. C., Hutchinson J. W. (1997), Steady-State Crack Growth and Work of Fracture for Solids Characterized by Strain Gradient Plasticity, *J. Mechanics and Physics of Solids*, 45, 8, 1253–1273.

Yoshida T., Tatsuoka F., Siddiquee M. (1994), Shear Banding in Sands Observed in Plane Strain Compression, *Localisation and Bifurcation Theory for Soils and Rocks.* In: R. Chambon, J. Desrues and I. Vardoulakis, editors, 165–181, Balkema, Rotterdam.

Zbib H., Aifantis E. (1988a), On the Localisation and post Localisation of Plastic Deformation, Part 1, On the Initiation of Shear Bands, *Res. Mechanica*, 23, 261–277.

Zbib H., Aifantis E. (1988b), On the Localisation and Post Localisation of Plastic Deformation, Part 1, On the Evolution and Thickness of Shear Bands, *Res. Mechanica*, 23, 279–292.

Zbib H. M., Rhee M., Hirth J. P. (1998), On Plastic Deformation and the Dynamics of 3D Dislocations, *Int. J. Mech. Sci.*, 40, 113–127.

Zervos Z., Papanastasiou P., Vardoulakis I. (2001), A Finite Element Displacement Formulation for Gradient Plasticity, *Int. J. Numer. Methods in Engineering,* 50, 1369–1388.

Zhou W., Zhao J., Liu Y., Yang Q. (2002), Simulation of Localization with Strain-Gradient-Enhanced Damage Mechanics, *Int. J. Num. And Anal. Meth. Geomech.,* 26, 793–813.